Raman Spectroscopy of the *Ff* Gene V Protein and Complexes with Poly(dA): Nonspecific DNA Recognition and Binding†

James M. Benevides,‡ Thomas C. Terwilliger,§ Stanislav Vohník,‡ and George J. Thomas, Jr.*,‡

Division of Cell Biology and Biophysics, School of Biological Sciences, University of Missouri−Kansas City, Kansas City, Missouri 64110, and Structural Biology Group, Mail Stop M888, Los Alamos National Laboratory, Los Alamos, New Mexico 87545

Received November 2, 1995; Revised Manuscript Received May 16, 1996⊗

ABSTRACT: Raman spectra of crystals and solutions of the single-stranded DNA binding protein of bacteriophage *Ff* (gene V protein, gVp) and of solution complexes of gVp with single-stranded poly(deoxyadenylic acid) [poly(dA)] reveal the following: (i) The gVp secondary and tertiary structures are similar in solution and in the crystal and are dominated by β-sheet domains, in agreement with NMR and X-ray findings. (ii) Subunit conformation and side chain environments of gVp are virtually unchanged over a wide range of salt concentration ($0 <$ [NaCl] < 100 mM); however, the solution conformation of poly(dA) exhibits sensitivity to added salt. The perturbed Raman markers indicate subtle changes in helix backbone geometry with accompanying small differences in base stacking as the concentration of NaCl is changed. (iii) In complexes with poly(dA), neither the conformation of gVp nor its side chain environments are altered significantly in comparison to the free protein. This is the case at both high salt (nucleotide-to-subunit binding stoichiometry $n = 4$) and low salt ($n = 3$). (iv) The Raman signature of poly(dA) undergoes small perturbations upon gVp binding, indicative of small changes in base stacking and phosphodiester backbone conformation. The present results show that the different stoichiometric binding modes of gVp to poly(dA) are accomplished without significant changes in gVp subunit structure and with only modest changes in the single-stranded poly(dA) ligand. This contrasts sharply with sequence-specific double-stranded DNA binding proteins, such as the phage lambda and D108 repressors, which undergo substantial structural changes upon DNA binding, and which also alter more dramatically the Raman fingerprints of their DNA target sites. Thus, nonspecific and specific nucleic acid recognition modes are distinguishable by Raman spectroscopy. The Raman signature of gVp also allows examination of hydrogen bonding interactions of unique side chains within the hydrophobic core (cysteine 33) and at the binding interface (tyrosine 41). These are discussed in relation to the recently published gVp crystal structure.

The gene V protein (gVp)[1] of *Ff* filamentous viruses (*fd*, *f1* and *M13*) plays a central role in the life cycle of the phage (Model & Russel, 1988). Dimers of gVp bind nonspecifically, cooperatively, and with high affinity to the viral single-stranded DNA (ssDNA) genome to promote the change from synthesis of the double-stranded replicative form to the ssDNA form. In addition, gVp functions as a repressor by regulating the expression of several phage-encoded proteins (Zaman *et al.*, 1990, 1991). However, the molecular mechanism by which gVp binds to genomic ssDNA is not known.

Owing to its relatively small size (87 amino acids; sequence, MIKVEIKPSQAQFTTRSGVS RQGKPYSLNE QLCYVDLGNE YPVLVKITLD EGQPAYAPGLYTVHLSSFKV GQFGSLMIDR LRLVPAK) and high solubility, gpV has been amenable to both X-ray crystallographic and NMR spectroscopic examinations. [The recent literature has been surveyed by Olah *et al.* (1995).] However, a three-dimensional structure has been determined only for the free protein dimer in the absence of ssDNA (Folkers *et al.*, 1994; Skinner *et al.*, 1994; Guan *et al.*, 1994; Brayer & McPherson, 1983). Although gVp binds a wide range of nucleic acids, no complex has yet proved suitable for high-resolution structure determination.

Raman spectroscopy is well suited to probing the structures of nucleoprotein complexes (Thomas & Tsuboi, 1993). Studies of several repressor−operator systems (Benevides *et al.*, 1991a,b, 1994a,b) provide a basis for comparing and contrasting the structural principles involved in nonspecific and specific DNA recognition. Here, we employ Raman spectroscopy to investigate the solution and crystal structures of gVp alone and in complexes with poly(deoxyadenylic acid) [poly(dA)], which serves as a model for the nonpaired domains of ssDNA. The gVp crystals examined here have yielded the 1.8 Å X-ray structure of Skinner *et al.* (1994). Complexes in solution have been examined at conditions comparable to the two stoichiometric binding modes distinguished by circular dichroism (CD) and fluorescence spectroscopic measurements (Kansy *et al.*, 1986; Bulsink *et al.*, 1988). The two complexes are believed to differ in the number, *n*, of nucleotides per protein subunit. The $n = 4$

† Part LIII in the series Structural Studies of Viruses by Raman Spectroscopy. Supported by NIH Grant GM50776 (G.J.T.).

* Author to whom correspondence may be addressed.

‡ University of Missouri−Kansas City.

§ Los Alamos National Laboratory.

⊗ Abstract published in *Advance ACS Abstracts,* July 1, 1996.

[1] Abbreviations: gVp, gene V protein common to the *Ff* bacteriophages (*fd*, *f1*, and *M13*); poly(dA), poly(deoxyadenylic acid); dsDNA, double-stranded DNA; ssDNA, single-stranded DNA; PEG, poly(ethylene glycol).

S0006-2960(95)02602-X CCC: $12.00

binding mode is favored by high ionic strength, while the $n = 3$ mode is favored by low ionic strength.

The present results are discussed in relation to recently proposed molecular models for gVp/ssDNA complexes (Guan *et al.*, 1994, 1995; Skinner *et al.*, 1994; Olah *et al.*, 1995).

EXPERIMENTAL PROCEDURES

1. Materials. Gene V protein was isolated and purified as described (Liang & Terwilliger, 1991). Crystals (space group *C2*) were obtained by vapor diffusion using a hanging drop method (Skinner *et al*., 1994). The crystallization buffer contained 10 mM Tris-HCl, pH 7.5, and 12% poly(ethylene glycol) (PEG).

PEG-3400 was obtained from Aldrich Chemical Co. (St. Louis, MO). Poly(dA) and other reagents were obtained from Sigma Chemical Co. (St. Louis, MO).

2. Raman Spectroscopy. Samples of gVp and its complexes with poly(dA) were brought to a final protein concentration of 65 mg/mL in 8 mM Tris, pH 7.2 ± 0.1, using an Amicon concentrator. The salt concentration was adjusted by the addition of 0.5 M NaCl. Poly(dA) was dissolved to 36 mg/mL in 8 mM Tris, pH 7.2 ± 0.1.

Solutions of gVp, poly(dA), and complexes were sealed in glass capillary cells (Kimax no. 34507) and thermostated at 10 °C during Raman data collection protocols. Spectra in the region from 560 to 1760 cm^{-1} were excited with the 514.5 nm line of an argon laser (Innova Model 70; Coherent, Inc., Santa Clara, CA) and were collected on a triple spectrometer (Model 1877; Spex Industries, Princeton, NJ) equipped with a liquid-nitrogen-cooled charge-coupled-device detector (Princeton Instruments, Princeton, NJ). Typically, 10 exposures of 120 s duration were accumulated and averaged to generate the Raman spectra presented below. Spectrometer slits were adjusted to achieve a spectral resolution of approximately 6 cm^{-1}. Raman frequencies of well-resolved bands are accurate to within ±1.0 cm^{-1}, and those of weak and/or broad bands are accurate to ±3 cm^{-1}.

Solvent background was corrected by computer subtraction techniques described previously (Benevides *et al.*, 1984). The Raman band at 1450 cm^{-1} (methylene deformation) was employed for normalization of gVp difference spectra, and the Raman band near 1092 cm^{-1} (phosphodioxy group) was employed for normalization of spectra of poly(dA) and complexes. The basis for this normalization has been described (Benevides *et al.*, 1991a).

Raman spectra of gVp and its complexes with poly(dA) in the S−H stretching region (2300−2700 cm^{-1}) were recorded on a Ramalog 1401 spectrometer (Spex Industries) equipped with a Model R298P photomultiplier (Hamamatsu, Tokyo). Data were collected at 0.5 cm^{-1} intervals with a spectral resolution of 8 cm^{-1} and an integration time of 3 s. Thirty or more scans were accumulated and averaged.

Spectra of gVp single crystals thermostated at 5 °C were obtained on a Raman microspectrophotometer consisting of an Innova argon laser (Coherent, Inc.), Model BHSM light microscope with Model ULWD MS plan 80X objective (Olympus, Inc.), Model S3000 triple spectrograph (Jobin-Yvon, Princeton, NJ), and Spectraview 2D charge-coupled-device detector (ISA, Inc., Princeton, NJ). Further details of this instrumentation have been described (Benevides *et al.*, 1993). Raman spectra in the 180° scattering geometry were collected for two crystal orientions, i.e., with the long axis of the crystal either parallel or perpendicular to the electric vector of the incident radiation (514.5 nm). The radiant power at the sample was less than 15 mW. Raman data, collected for the spectral regions 500−1800 cm^{-1} and 2300−2700 cm^{-1}, are presented below as unsmoothed averages of 6−10 exposures, each obtained with an integration time of 120 s/exposure and spectral resolution of approximately 6 cm^{-1}. Spectra of the mother liquor and crystal were obtained at identical conditions, and the former was subtracted from the latter as previously described (Benevides *et al.*, 1984).

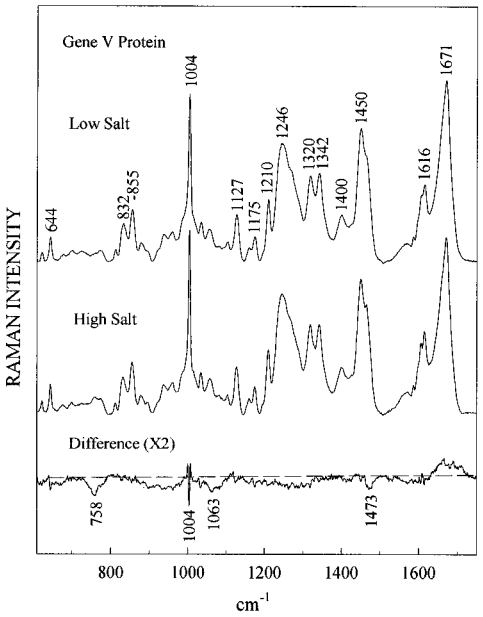

FIGURE 1: Raman spectra in the region 600−1750 cm^{-1} of gVp at 65 $\mu g/\mu L$ in 8 mM Tris, pH 7.2 (low-salt buffer, top), and 8 mM Tris, pH 7.2, 100 mM NaCl (high-salt buffer, middle), and a 2-fold amplification of their difference spectrum (low salt minus high salt, bottom).

RESULTS

1. Gene V Protein. Because differentiation between the $n = 4$ (high salt) and $n = 3$ (low salt) modes of gVp binding to ssDNA can be achieved by adjusting the NaCl concentration, we examined the Raman spectrum of the free protein in 8 mM Tris-HCl, both with and without 100 mM NaCl (Kansy *et al.*, 1986). The gene V protein binds cooperatively to poly(dA) with a binding constant that is large and salt-dependent. The effective binding constant [denoted $K_{int}w$ by Kansy *et al.* (1986)] is $\approx 10^6$ M^{-1} in 150 mM NaCl, and $> 10^9$ M^{-1} in 10 mM NaCl. Therefore, in the present study, which employs gVp at approximately 7 mM and with a 4:1 ratio of nucleotides:gVp monomer, virtually all of the protein is bound to nucleic acid. This is true in both the absence and presence of added 100 mM NaCl. [In the latter case, the total Na^+ concentration, including poly(dA) counterions, remains below 150 mM.] Raman spectra of gVp obtained at low- and high-salt conditions and their difference spectrum, computed with the low-salt spectrum as minuend, are shown in Figure 1. Assignments for the Raman bands are given in Table 1. We find that the Raman spectrum, and therefore the solution conformation of gVp, is essentially insensitive to NaCl. The very weak features in the difference

Table 1: Raman Frequencies, Intensities, and Assignments of the *fd* Gene V Protein

frequency (cm^{-1})	relative intensity[a]	assignment[b]
623	0.5	F
644	1.2	Y
677	0.3	C
700	0.5	M; amide IV
725	0.5	M
758	0.4	F
773	0.6	−
812	0.6	−
832	2.0	Y
855	2.9	Y, I, L
879	1.0	G
894	0.6	G, S
923	0.7	K, I, E, D,
937	1.5	K [CN str, CNC_α def]
960	1.6	V, L [CH_3 sym rock, op]
985	2.3s	I
1004	9.2	F
1013	2.4s	−
1035	2.1	F, Y, G, S, V
1057	1.8	K, E, F, S
1081	0.8	E, F
1127	2.5	V, L, I, E, D, G [CC str]
1160	0.8	A, L [CH_3 asym rock, ip]
1175	1.4	V, L, A [CH_3 asym rock, op]; Y
1210	3.4	Y, F
1246	6.5	amide III [β-strand]
1269	5.0	Y, amide III [α-helix]
1320	4.7	K, I [CH_2 twist/wag]; [$C_\alpha H$ def]
1342	4.9	K, I, L [CH_2 twist/wag], S, G; amide III [α-helix]
1400	2.6	E, D
1450	7.4	I, L, K, S [CH_2 scissor]
1465	5.8	I, L, V, A [CH_3 def]
1569	0.9b	−
1587	1.4	F
1606	3.7	F, Y
1616	4.3	Y
1671	10.0	amide I [β-strand]

[a] Relative peak height on 0−10 scale (Figure 1). [b] Assignments are based upon model proteins [reviewed by Miura and Thomas (1995)]; one-letter symbols indicate amino acids; brackets indicate chemical subgroups; other abbreviations: str, stretching; def, deformation; sym, symmetric; asym, asymmetric; ip, in-phase; op, out-of-phase.

spectrum of Figure 1 (bottom trace) can be attributed to imperfect compensation of Raman bands of the Tris buffer (troughs at 758, 1063, and 1473 cm^{-1}) and to a base line artifact above 1620 cm^{-1}. Raman marker bands diagnostic of protein secondary structure (amide I at 1671 cm^{-1} and amide III at 1246 cm^{-1}) and side chain environments (Table 1) are essentially unaffected by NaCl. The sole apparent exception is a slight broadening of the 1004 cm^{-1} marker of phenylalanine. This small change in bandshape may signify that Phe environments are slightly more uniform at the high-salt condition. The positions of amide I and amide III markers in Figure 1 identify the β-sheet as the predominant secondary structure of gVp in solution (Chen & Lord, 1974). This result is in accord with the X-ray crystal structure (Skinner *et al.*, 1994).

2. Poly(deoxyadenylic acid). Raman spectra of poly(dA) in low and high-salt solutions and their corresponding difference spectrum are shown in Figure 2. Detailed band assignments have been given elsewhere (Small & Peticolas, 1971; Thomas & Benevides, 1985). In contrast to gVp, the structure of poly(dA) is sensitive to salt. The positive difference peaks near 983 and 1223 cm^{-1} and troughs near

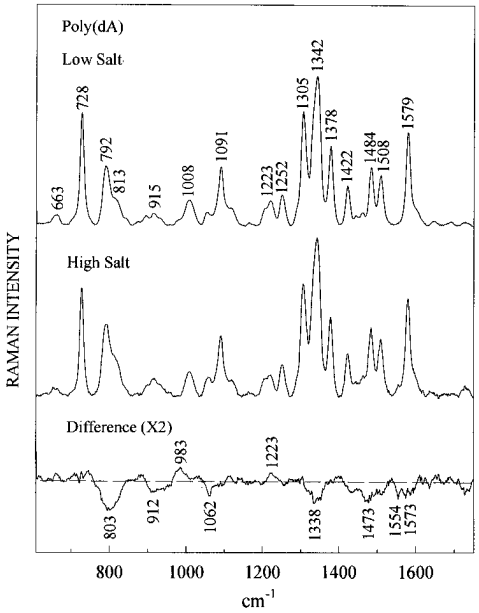

FIGURE 2: Raman spectra in the region 600−1750 cm^{-1} of poly(dA) at 40 $\mu g/\mu L$ in low-salt buffer (top), high-salt buffer (middle), and a 2-fold amplification of their difference spectrum (low salt minus high salt, bottom). Buffers are as described in Figure 1.

1338, 1473, 1554, and 1573 cm^{-1} are due to the base residue and presumably indicate altered base environments with the change in NaCl. The troughs at 803 and near 912 and 1062 cm^{-1} are attributed to the phosphodiester moiety and indicate a subtle effect of NaCl on helix backbone geometry. The most prominent effects, *viz.*, intensity increases near 803 cm^{-1} and 1338 cm^{-1}, parallel those induced in poly(dA-dT)·poly(dA-dT) by changes in relative humidity (Thomas & Benevides, 1985). A salt-induced structural change in poly(dA) may play a role in the mechanism of gVp binding. Although the present spectra do not identify the number of different chain conformations contributing to the low-salt and high-salt forms of poly(dA), the data indicate clearly that the average structure is altered by the change in NaCl concentration.

3. Complex of gVp and Poly(dA) at Low Salt: gVp/Poly(dA)$_L$. Figure 3 compares the Raman spectrum of the low-salt complex [gVp/poly(dA)$_L$, top trace] with the spectral sum of its components (middle trace). The computed difference spectrum (bottom trace) exhibits many peaks and troughs, indicating that the Raman signature of gVp/poly(dA)$_L$ is not simply the sum of its constituents. Most of the difference bands match the positions of peaks in the poly(dA) spectrum and therefore are probably due to poly(dA). Accordingly, the majority of structural perturbations associated with the formation of gVp/poly(dA)$_L$ occur in the poly(dA) ligand. These perturbations can be explained in terms of altered base environments (719−732 cm^{-1} and 1290−1590 cm^{-1} regions) and conformational changes of the polynucleotide backbone (Raman difference bands near 792, 990, and 1099 cm^{-1}).

Bands in the Figure 3 difference spectrum at 937, 1292, and 1663 cm^{-1} are consistent with protein assignments (Table 1). However, their extremely low intensities indicate that only marginal perturbations occur in the gVp structure upon complex formation. For example, the putative amide I trough (1663 cm^{-1}) represents less than 5% of the parent band intensity, suggesting that no more than a few peptide residues

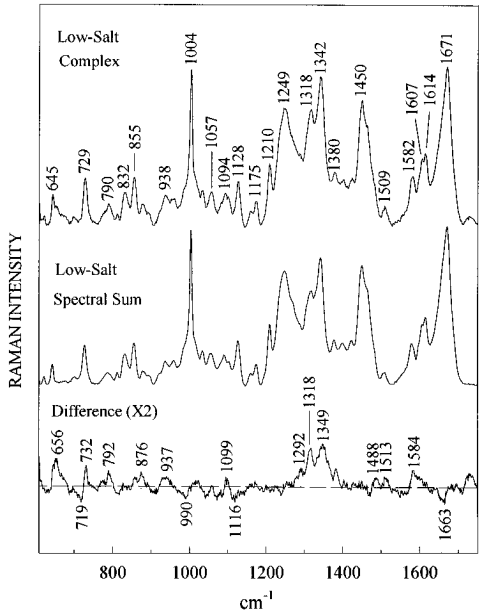

FIGURE 3: Raman spectrum in the region 600−1750 cm^{-1} of the gVp/poly(dA) complex in low-salt buffer (top), the spectral sum of constituents (middle), and a 2-fold amplification of their computed difference spectrum (bottom). In this complex, the nucleotide-to-subunit binding stoichiometry is believed to be 3:1 (Kansy *et al.*, 1986).

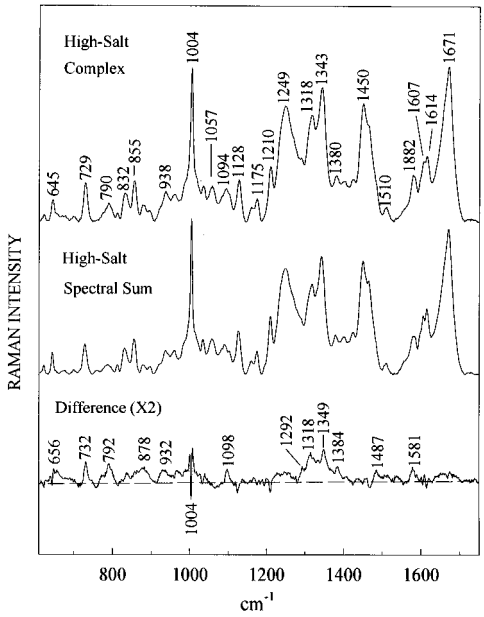

FIGURE 4: Raman spectrum in the region 600−1750 cm^{-1} of the gVp/poly(dA) complex in high-salt buffer (top), the spectral sum of constituents (middle), and a 2-fold amplification of their computed difference spectrum (bottom). In this complex, the nucleotide-to-subunit binding stoichiometry is believed to be 4:1 (Kansy *et al.*, 1986).

can be perturbed conformationally by poly(dA) binding. Protein side chain packing is also essentially invariant to poly(dA) binding. For example, in aqueous gVp the intensity ratio I_{855}/I_{832} of the tyrosine Fermi doublet at 855 and 832 cm^{-1}, which is diagnostic of tyrosine phenoxyl hydrogen bonding states (Siamwiza *et al.*, 1975), is unchanged by complex formation.

4. Complex of gVp and Poly(dA) at High Salt: gVp/Poly-(dA)$_H$. Comparison with the Low-Salt Complex. Figure 4 compares the Raman spectrum of the high-salt complex [gVp/poly(dA)$_H$, top trace] with the spectral sum of its

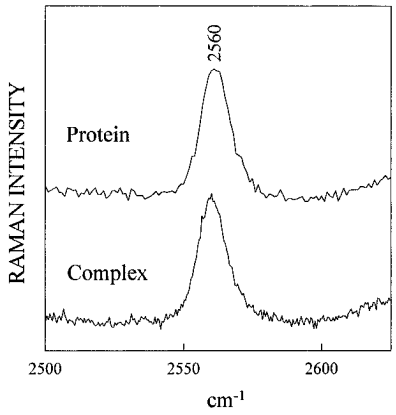

FIGURE 5: Raman spectra in the S−H stretching region (2500−2625 cm^{-1}) of gVp (top) and the gVp/poly(dA) high-salt complex (bottom), each obtained in solution containing 8 mM Tris, pH 7.2, + 100 mM NaCl.

constituents (middle trace). The corresponding difference spectrum (bottom trace) is again dominated by bands of poly-(dA). Accordingly, the majority of structural perturbations associated with the formation of gVp/poly(dA)$_H$ occur in the poly(dA) ligand. Again, these perturbations can be explained in terms of altered base environments and conformational changes of the polynucleotide backbone. Further interpretation is given in the Discusssion.

Interestingly, the difference spectrum of Figure 4 closely parallels that of Figure 3, indicating that at both high and low salt the poly(dA) spectrum is perturbed similarly by gVp binding. This close correspondence between difference spectra of Figures 3 and 4 provides direct experimental evidence that the nature of interactions between gVp and poly(dA) is similar for both salt environments even though the initial conformations of poly(dA) are detectably different (*cf.* Figure 2).

The above findings suggest that upon binding to a given ssDNA structure the gVp molecules largely conserve the preexisting conformation(s). This is demonstrated by the present data for two distinct ssDNA environments, the low-salt and high-salt forms of poly(dA), and is presumably the case for other ssDNA environments as well. Such nonspecificity of gVp binding with respect to the initial ssDNA structure may be facilitated by diversity in the binding stoichiometry. The mechanism of gVp binding evidently involves an accommodation of the architecture of the DNA ligand rather than imposition of major structural changes upon it. Thus, the solution salt concentration does not appear to play a major role in determining the structural details of the gVp/ssDNA complex.

5. Environment of Cysteine 33. The Raman band corresponding to the sulfhydryl (S−H) stretching vibration is highly sensitive to the sulfhydryl local environment. Markers have been identified for strongly hydrogen-bonded cysteine S−H donors at 2525−2560 cm^{-1}, for moderate donors at 2560−2575 cm^{-1}, and for weak donors at 2575−2580 cm^{-1} (Li & Thomas, 1991; Li *et al.*, 1992). Figure 5 shows that the Raman S−H marker for gVp occurs at 2560 cm^{-1} in both the free protein and the low-salt complex, indicating that the S−H group of the cysteine 33 (Cys33) side chain is at least moderately hydrogen bonded. Because this hydrogen bonding state is unaffected by gVp binding to poly(dA), the Cys33 side chain evidently does not participate in ssDNA recognition. The present finding is

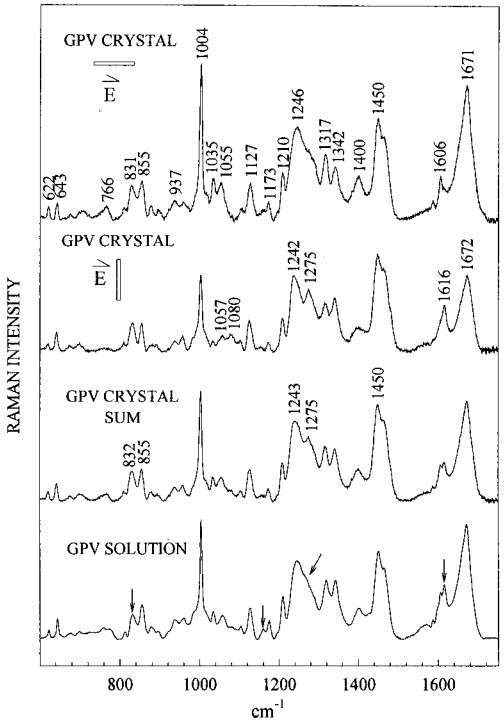

FIGURE 6: Raman spectra in the region 600−1750 cm^{-1} of a gVp single crystal oriented with the long axis (crystallographic *b* axis) of the crystal parallel to the electric vector of the incident laser beam (top), with the long axis perpendicular to the electric vector of the incident laser beam (second from top), the sum of the top two spectra (second from bottom), and the high-salt solution spectrum of gVp (bottom). Arrows in the bottom spectrum indicate bands exhibiting large intensity differences between crystal and solution.

consistent with the location of Cys33 in the interior of the gVp tertiary structure (Skinner *et al.*, 1994).

The position of the Raman S−H marker at 2560 cm^{-1} was somewhat unexpected because the gVp crystal structure reveals no definitive hydrogen bond acceptor in the vicinity of the S−H donor (Skinner *et al.*, 1994). One explanation is that the putative acceptor (e.g., an H_2O molecule) is not sufficiently ordered to be detected in the electron density map.

6. Raman Spectroscopy of the gVp Crystal Structure. The versatility of Raman spectroscopy allows comparison of the molecular structures of gVp in crystal and solution states. We obtained the Raman spectrum of a statically oriented gVp single crystal of the same morphology and in the same mother liquor as employed previously for X-ray analysis (Skinner *et al.*, 1994). Figure 6 compares Raman spectra in the region 600−1750 cm^{-1} excited with the electric vector of the incident laser radiation parallel (top trace) and perpendicular (second trace from top) to the crystallographic *b* axis of the gVp single crystal. Corresponding data for the S−H stretching region of the Raman spectrum are shown in Figure 7. The different Raman intensity patterns observed for these two configurations of the crystal are typical of a single-crystal Raman spectrum in which the molecules are oriented with respect to the laser electric vector (Thomas & Tsuboi, 1993). To provide a comparison of the single-crystal data of Figure 6 with the solution Raman spectrum (corresponding to randomly oriented molecules), the parallel and perpendicular spectra were added together to simulate a more "random" collection of gVp molecules in the crystalline state. This summation spectrum is included in Figure 6 (second trace from bottom) and is seen to agree rather closely in band frequencies and relative intensities with the solution spectrum (bottom trace). Nonetheless, some important differences exist.

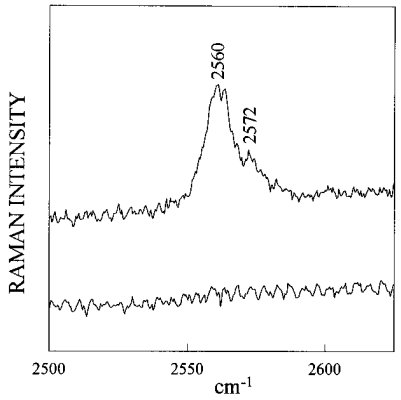

FIGURE 7: Raman spectra in the S−H stretching region (2500−2625 cm^{-1}) of a gVp single crystal oriented with the crystallographic *b* axis parallel (top) and perpendicular (bottom) to the electric vector of the incident laser beam.

The arrows in the bottom spectrum of Figure 6 identify the Raman bands of the gVp solution which differ most significantly in intensity from the corresponding bands of the crystal. The band at 1275 cm^{-1}, which is more prominent in the crystal than in solution, is assigned to tyrosine residues (Overman & Thomas, 1995) and not to amide III. This is consistent with the invariance of amide I at 1671 cm^{-1}, indicating that the subunit secondary structure is not sensitive to the solvent or crystal environment and therefore no amide III change should occur. It is also consistent with the substantial sensitivity of other tyrosine marker bands (arrows, Figure 6) to gVp environment. For example, the tyrosine Fermi doublet at 832 and 855 cm^{-1} exhibits an intensity ratio $I_{855}/I_{832} = 1.40 \pm 0.05$ in solution, which is much greater than the ratio observed in either the parallel or the perpendicular crystal spectrum. For comparison with the solution spectrum, the summation crystal spectrum provides the value $I_{855}/I_{832} \approx 1.1$. This indicates that the average hydrogen bonding state for tyrosine phenoxyls differs significantly between the solution and crystal environments (Siamwiza *et al.*, 1975). A change of I_{855}/I_{832} from 1.4 to 1.1 is expected if one of the five phenoxyls undergoes a major change in hydrogen bonding state. Further discussion in terms of tyrosine environments in the X-ray structure is given in the Discussion.

In principle, the polarized Raman intensity ratio can be exploited to determine orientations of specific molecular subgroups in the crystal lattice (Thomas & Tsuboi, 1993). However, such determinations require prior knowledge of the corresponding Raman scattering tensors, and these are generally not known. Conversely, information about a local Raman tensor can be obtained from the polarized Raman intensity ratio if the orientation of the molecular subgroup which gives rise to the Raman band is known (Benevides *et al.*, 1993). In the *C2* crystal structure, each gVp subunit is oriented so that the S−H bond of Cys33 is directed nearly parallel to the crystallographic *b* axis (Skinner *et al.*, 1994). Accordingly, the vanishingly low intensity of the S−H band in the perpendicular spectrum of Figure 7 provides evidence of a highly anisotropic Raman tensor for the S−H vibration, wherein the largest component of the tensor principal axis is directed along the S−H bond.

Figure 7 also shows that, as in the case of the gVp solution, the S−H marker occurs in the crystal at 2560 cm^{-1}. This indicates that the S−H group of Cys33, which is in the interior of the five-stranded β-barrel, has the same hydrogen bonding environment in both the crystal and solution structures. (The satellite band at 2572 cm^{-1}, which is not observed in the solution spectrum, is assigned to an overtone or combination mode. One candidate is the overtone of the C−S−H deformation mode, for which the fundamental is expected in the 1200−1300 cm^{-1} region.)

DISCUSSION

The Raman spectrum of gVp is consistent with both X-ray (Skinner *et al.*, 1994) and high-resolution multidimensional NMR (Folkers *et al.*, 1994) studies which have established the β-strand as the predominant secondary structure of the protein subunit. The Raman data show further that the secondary and tertiary structures of gVp are minimally affected by salt concentration in the range 0 < [NaCl] < 100 mM, despite evidence that in this range of NaCl concentration the stoichiometry of gVp binding to poly(dA) is altered (Kansy *et al.*, 1986). On the other hand, the Raman spectrum of poly(dA) is more significantly perturbed by NaCl concentration. The salt-induced structural change in poly(dA) may also play a role in the mechanism of gVp binding. Although the present spectra do not identify the number of different chain conformations contributing to the low-salt and high-salt forms of poly(dA), the data indicate clearly that the overall conformer population is changed by the change in NaCl concentration. The results suggest that the source of versatility in the DNA binding stoichiometry of gVp may reside either in the polynucleotide ligand itself or in a property of the nucleoprotein complex not shared by the gVp subunit alone.

Raman spectra of gVp/poly(dA) complexes at low and high salt indicate that the protein structure does not change significantly upon binding to initially different poly(dA) conformations. The capability of gVp to recognize and bind different ssDNA secondary structures while essentially conserving its structure contrasts sharply with the case of prokaryotic gene regulatory complexes previously examined by Raman spectroscopy (Benevides *et al.*, 1991a,b, 1994a,b). The bacteriophage repressor structures are appreciably affected by binding to double-helical DNA. For example, in the case of the cI repressor of bacteriophage lambda, differences in the hydrogen bonding states of tyrosine side chains are evident upon binding to the O_L operator site. Similarly, structural change is propagated through the DNA duplex. Specific side chains of the repressor and specific base and backbone sites in the DNA operator are involved in hydrogen bonding, and these specific interactions are evident in the Raman spectra (Benevides *et al.*, 1991a,b, 1994b). In contrast, gVp binding to poly(dA) does not produce significant changes in the Raman signature of the protein, and the changes identified in the spectrum of the polynucleotide ligand are not a sensitive function of the binding stoichiometry. Putative hydrogen bonding interactions of poly(dA) bases with gVp side chains are apparently not sufficiently strong or extensive to be detected by Raman spectroscopy.

Previous studies of gVp have suggested that binding to ssDNA involves hydrogen bonding contacts between basic side chains (lysine and arginine) and DNA phosphates. While small Raman intensity changes attributable to the DNA backbone are observed (792 and 820−880 cm^{-1}), these are much smaller than those accompanying specific binding of bacteriophage repressors to their operator sites (Benevides *et al.*, 1994a,b). In the latter cases, protein binding significantly and specifically perturbs the DNA structure.

A model for the gVp/ssDNA complex has been proposed recently by Guan *et al.* (1995) on the basis of X-ray structures of wild-type and mutant (Y41H) forms of the free protein (Skinner *et al.*, 1994; Guan *et al.*, 1994). The model assumes that the structure of the complex is essentially independent of binding stoichiometry; i.e., $n = 3$ and $n = 4$ complexes are not distinguished by qualitatively different contacts between gVp subunits and nucleotide residues. The present experimental results are consistent with that proposal. The model also assumes that the three-dimensional structure of gVp is largely unchanged upon complex formation with ssDNA, which is again supported by the present experimental results.

Structural details of the model of Guan *et al.* (1995) include a left-handed helix with 32 bases per helical turn and pitch of 90 Å. On the other hand, previous studies of poly(dA) in solution (Olsthoorn *et al.*, 1980) are consistent with a right-handed helix of 9 bases per turn and pitch of 25 Å. Although the axial rise per base is identical (≈2.8 Å) in the two models (90 Å/32 bases, 25 Å/9 bases), the handedness and helical twist (40° vs ≈11.2°) are very different. Of course, these structural details are not probed directly by the Raman spectra. Yet, the present results suggest that the backbone conformation of poly(dA), as well as adenine base stacking, is only moderately perturbed by gVp binding. The Raman results further suggest that the final structure of DNA in the complex does not differ greatly from its structure in the absence of gVp. A logical starting point for modeling the gVp/ssDNA complex would appear to be the solution conformation of poly(dA).

Finally, in the gVp/ssDNA model of Guan *et al.* (1995), it has been proposed that dimers of gVp are linked in the left-handed superhelix by contact loops similar to those involving tyrosine in the $P2_12_12_1$ crystal of the free protein (Guan *et al.*, 1994). Our results indicate that while tyrosine hydrogen bonding environments are conserved between free and complexed states of gVp in solution, they are not conserved between the solution and *C2* crystalline forms of the free protein. This suggests a need for caution in employing the dimer packing arrangement observed in the $P2_12_12_1$ crystal structure as a basis for elucidating the organization of the gVp/ssDNA complex in solution.

REFERENCES

Benevides, J. M., Wang, A. H.-J., van der Marel, G. A., van Boom, J. H., Rich, A., & Thomas, G. J., Jr. (1984) *Nucleic Acids Res. 12*, 5913−5925.
Benevides, J. M., Weiss, M. A., & Thomas, G. J., Jr. (1991a) *Biochemistry 30*, 4381−4388.
Benevides, J. M., Weiss, M. A., & Thomas, G. J., Jr. (1991b) *Biochemistry 30*, 5955−5963.
Benevides, J. M., Tsuboi, M., & Thomas, G. J., Jr. (1993) *J. Am. Chem Soc. 115*, 5351−5359.
Benevides, J. M., Kukolj, G., Autexier, C., Aubrey, K. L., DuBow, M., & Thomas, G. J., Jr. (1994a) *Biochemistry 33*, 10701−10710.
Benevides, J. M., Weiss, M. A., & Thomas, G. J., Jr. (1994b) *J. Biol. Chem. 629*, 10869−10878.
Brayer, G. D., & McPherson (1983) *J. Mol. Biol. 169*, 565−596.

Bulsink, H., Harmsen, B. J. M., & Hilbers, C. W. (1988) *Eur. J. Biochem. 176*, 597−608.
Chen, M. C., & Lord, R. C. (1974) *J. Am. Chem. Soc. 96*, 4750−4752.
Folkers, P. J. M., Nilges, M., Folmer, R. H. A., Konings, R. N. H., & Hilbers, C. W. (1994) *J. Mol Biol. 236*, 229−246.
Guan, Y., Zhang, H., Konings, R. N. H., Hilbers, C. W., Terwilliger, T. C., & Wang, A. H.-J. (1994) *Biochemistry 33*, 7768−7778.
Guan, Y., Zhang, H., & Wang, A. H.-J. (1995) *Protein Sci. 4*, 187−197.
Kansy, J. W., Clack, B. A., & Gray, D. M. (1986) *J. Biomol. Struct. Dyn. 3*, 1079−1110.
Li, H., & Thomas, G. J., Jr. (1991) *J. Am. Chem. Soc. 113*, 456−462.
Li, H., Wurrey, C. J., & Thomas, G. J., Jr. (1992) *J. Am. Chem. Soc. 114*, 7463−7469.
Liang, H., & Terwilliger, T. C. (1991) *Biochemistry 30*, 2772−2782.
Miura, T., & Thomas, G. J., Jr. (1995) in *Subcellular Biochemistry, Volume 24, Proteins: Structure, Function, and Engineering* (Biswas, B. B., & Roy, S., Eds.) pp 55−99, Plenum Press, New York.
Model, P., & Russel, M. (1988) in *The Bacteriophages* (Calendar, R., Ed.) pp 2099−2107, Plenum, New York.
Olah, G. A., Gray, D. M., Gray, C. W., Kergil, D. L., Sosnick, T. R., Mark, B., Vaughan, M. R., & Trewhella, J. (1995) *J. Mol. Biol. 249*, 576−594.
Olsthroon, C. S. M., Bostelaar, L. J., van Boom, J. H., & Altona, C. (1980) *Eur. J. Biochem. 112*, 95−110.
Overman, S. A., & Thomas, G. J., Jr. (1995) *Biochemistry 34*, 5440−5451.
Siamwiza, M. N., Lord, R. C., Chen, M. C., Takamatsu, T., Harada, I., Matsuura, H., & Shimanouchi, T. (1975) *Biochemistry 14*, 4870−4876.
Skinner, M. M., Zhang, H., Leschnitzer, D. H., Guan, Y., Bellamy, H., Sweet, R. M., Gray, C. W., Konings, R. N. H., Wang, A. H.-J., & Terwilliger, T. C. (1994) *Proc. Natl Acad. Sci. U.S.A. 91*, 2071−2075.
Small, E. W., & Peticolas, W. L. (1971) *Biopolymers 10*, 69−88.
Thomas, G. J., Jr., & Benevides, J. M. (1985) *Biopolymers 24*, 1101−1105.
Thomas, G. J., Jr., & Tsuboi, M. (1993) *Adv. Biophys. Chem. 3*, 1−70.
Zaman, G. J. R., Schoenmakers, J. G. G., & Konings, R. N. H. (1990) *Eur. J. Biochem. 189*, 119−124.
Zaman, G. J. R., Smetsers, A., Kaan, A., Schoenmakers, J. G. G., & Konings, R. N. H. (1991) *Biochim. Biophys. Acta 1089*, 183−192.

BI952602E